Earthline Journal of Mathematical Sciences
E-ISSN: 2581-8147
Volume 14, Number 4, 2024, Pages 655-695
https://doi.org/10.34198/ejms.14424.655695

Causes of Backward Bifurcation in a Tuberculosis-Schistosomiasis Co-infection Dynamics

Ignatius Ako[1] and Owin Olowu[2,*]

[1] Department of Mathematics, University of Benin, Benin City, Nigeria
e-mail: ignatius.ako@uniben.edu

[2] Department of Mathematics, University of Benin, Benin City, Nigeria
e-mail: oghenewaire.olowu@uniben.edu

Abstract

To obtain a thorough understanding of the influence of schistosomiasis infections on the transmission dynamics of tuberculosis, a deterministic mathematical model for the transmission dynamics of tuberculosis (TB) co-infection with schistosomiasis is created and examined. The aim of the research is to examine the reasons behind the backward bifurcation in the co-infection dynamics of tuberculosis and schistosomiasis. The backward bifurcation phenomena can be caused by the following parameters, according to the model's analysis (when the associated reproduction number is less than one), other than the well established route of exogeneous re-infection of latently infected TB individuals, the relative rates at which humans with latent schistosomiasis (η_1) and active schistosomiasis (η_2) are infected with TB, respectively, the lowered rate of reinfection with schistosomiasis (ψ), the fraction of individuals who experience fast progression to active TB (p), the adjustment parameter which accounts for the increased probability of infectiousness of humans with active TB and latent schistosomiasis (Π_1), the treatment rate of people infected with active TB exposed to schistosomiasis (ζ_{T1}) and the rate of progression to active TB and exposed to schistosomiasis to active TB and active schistosomiasis (σ).

Received: February 28, 2024; Accepted: April 11, 2024; Published: May 1, 2024
2020 Mathematics Subject Classification: 93B99.
Keywords and phrases: tuberculosis, schistosomiasis, co-infection, backward bifurcation.
*Corresponding author

1 Introduction

Tuberculosis, popularly known as TB, precipitated by the pathogen *Mycobacterium tuberculosis*, taints a third of global populace, with the resultant consequence of two to three million fatalities annually [26, 48, 58], is a dominant health situation globally [59] that induces malady among several millions of persons annually and is positioned *paripasu* the human immunodeficiency virus (HIV) as a dominant agent of mortality globally [59]. It is estimated that 10% of persons infected with TB are disposed to advance to infectious TB [29]. There was a notification of 6.4 million fresh TB infections to governments and disclosed to WHO in 2017 [62]. The rate of success of medical care, in 2016, for humans freshly detected with the disease was reported to be 82% globally [62].

On the other hand, the prominence of schistosomiasis as a neglected tropical disease (NTD), ranks after malaria with respect to illness amongst humans in tropical regions of the world [24]. Schistosomiasis is induced by infectious parasitic flatworms of the class *Schistosoma* [24]. It was reported, in 2011, that 243 million persons living in 78 nations were estimated to be at high-risk for schistosomiasis in such territories [24]. Furthermore, according to WHO 2017 estimates, a minimum of 220.8 million people needed schistosomiasis preventive medical care with more than 102.3 million people reportedly treated [63]. The building of water projects to satisfy agricultural and power necessities for advancement have contributed immensely to rising infections [12, 31]. Constantly growing populace alongside migration, significantly, have supported increased infectiousness and appearance of the disease in uncharted frontiers [8, 12].

From the global reports on TB and schistosomiasis, respectively, above, it is evident that TB and schistosomiasis are co-endemic and co-infectious; and that the relevance of investigating if a pleura-residing parasitic worm can eventually frustrate the host's competence to contain pulmonary TB contagion will not be impaired [29, 45, 48, 58, 65]. The results from the works of [10, 29, 45, 48, 58], greatly suggest that infections from helminths adversely affects the host's capability to

regulate TB infection through a system involving substitute invigoration of pleura macrophages. Nonetheless, the systems resulting in the reactivation of TB in alternatively humans with effective immune systems are greatly obscured [29]. Per se, co-infection with parasitic worms is treated as a risk factor related along side enhanced susceptibility to tuberculosis and rates of tuberculosis reactivation [29].

Since the formulation of the first mathematical model for schistosomiasis by Macdonald [27], numerous authors have laboriously examined the disease dynamics of schistosomiasis through mathematical modeling geared towards control programmes for the disease. Particularly, [4, 14, 64] carried out extensive and detailed review of such schistosomiasis models. Of course, several authors have, indeed, further enriched the literature on the mathematical modelling of schistosomiasis since that time. [11, 13, 17, 18, 20–22, 28, 31, 32, 41–43, 49–51, 66, 67]. Furthermore, there have been several treatises on the mathematical investigation for the infection dynamics of TB [3, 5, 9, 16, 30, 34–40, 46, 53] since the pioneering work of Waaler *et al.* [57] was done. These other mathematical models formulated have given greater, deeper and clearer insights into TB population dynamics, thereby enhancing the literature. These other mathematical models formulated have given greater, deeper and clearer insights into TB population dynamics, thereby enhancing the literature. [31] formulated a model for the co-interaction of schistosomiasis and HIV/AIDS for the purpose of assessing their symbiotic connection in the company of therapeutic measures. [33] investigated, mathematically, malaria and schistosomiasis co-infection for the purpose of scrutinizing the symbiotic connection that exists between them in the presence of treatment.

From the preceding, it is obvious that divers mathematical models have been designed to analyze TB infection and schistosomiasis infection, respectively and their co-infections with other diseases but none has looked at the possibility of the co-infection dynamics of TB and schistosomiasis, to the best of the authors' awareness.

The document is categorized as follows: In Section 2, the model formulation

is presented. In Section 3, the qualitative mathematical analysis is completed along with the model's examination for the backward bifurcation phenomenon and global asymptotic stability (GAS) of the disease-free equilibrium (DFE). Section 4 provides a quantitative analysis of the model, and Section 5 provides a conclusion.

2 Model Formulation

The TB-schistosomiasis co-infection transmission model to be developed will assume the form of a system of non-linear deterministic differential equations. In the formulation, only populations (human beings, snails and intermediate stages of pathogen life-cycle (miracidia and cercariae)) directly involved in disease transmission dynamics are considered.

The model demarcates the entire human populace at time t, represented by $N_H(t)$, into fourteen mutually exclusive classes of susceptible to infections ($S_H(t)$), latent with TB but not infectious ($E_{HT}(t)$), active TB ($I_{HT}(t)$), exogenously re-infected with TB ($I_{RT}(t)$), treated for TB ($T_{HT}(t)$), exposed to schistosomiasis ($E_{HS}(t)$), with schistosomiasis infection ($I_{HS}(t)$), treated for schistosomiasis ($T_{HS}(t)$), exposed to TB, exposed to schistosomiasis ($E_{TS}(t)$), with active TB, schistosomiasis exposure ($I_{ST}(t)$), exogenously re-infected with TB, exposed to schistosomiasis ($I_{RS1}(t)$), exposed to TB, with active schistosomiasis ($E_{ST}(t)$), exogenously re-infected with TB and active schistosomiasis ($I_{RS2}(t)$), and with active TB, active schistosomiasis ($I_{TS}(t)$). Where

$$\begin{aligned} N_H(t) = {} & S_H(t) + E_{HT}(t) + I_{HT}(t) + I_{RT}(t) + T_{HT}(t) + E_{HS}(t) \\ & + I_{HS}(t) + T_{HS}(t) + E_{TS}(t) + I_{ST}(t) + I_{RS1}(t) + E_{ST}(t) \\ & + I_{RS2}(t) + I_{TS}(t). \end{aligned} \tag{2.1}$$

In order to include the pathogen that causes schistosomiasis in the co-infection dynamics, we assume that the cercariae and miracidia populations are represented by $L(t)$ and $J(t)$ classes respectively.

Next, we incorporate the intermediary hosts, freshwater snails, for the pathogen responsible for schistosomiasis in the model construction. We presume that the whole snail populace in the freshwater habitat at time t, given by $N_S(t)$, is categorized into the jointly exclusive classes of snails susceptible to infection ($S_S(t)$) along side snails infected with miracidia ($I_S(t)$), where

$$N_S(t) = S_S(t) + I_S(t). \tag{2.2}$$

All snails infected by miracidia, do not procreate as a result of castration [13, 31] and that periodic and climatic changes do not have any impact on the total number of snails and contact arrangements.

Θ_{RT} is an adjustment parameter accounting for the decreased probability of the transmission of TB by humans exogenously re-infected with TB, compared to persons with active TB [2]. The parameter Θ_{RS1} is a modification parameter accounting for the increased probability of the transmission of TB by humans exogenously re-infected with TB and exposed to schistosomiasis, compared to persons with active TB [54].

Based on the specific assumptions above, our developed model is represented by the following deterministic system of non-linear ordinary differential equations in (2.3); the corresponding variables and parameters of the model are tabulated in Table 1 and Table 2, respectively, while the values and ranges of the parameters used for numerical simulation on the model (2.3) are listed in Tables 3 and 4, respectively.

$$
\begin{aligned}
S'_H &= \Lambda_H - \lambda_T S_H - \lambda_J S_H - \mu_H S_H,\\
E'_{HT} &= (1-p)\lambda_T(S_H + \xi T_{HT} + T_{HS}) + \zeta_{S1} E_{ST} - (1-\pi_1)\lambda_T E_{HT}\\
&\quad - \lambda_J E_{HT} - (\kappa_1 + \mu_H) E_{HT},\\
I'_{HT} &= p\lambda_T(S_H + \xi T_{HT} + T_{HS}) + \kappa_1 E_{HT} + \zeta_{S3} I_{TS} - \lambda_J I_{HT}\\
&\quad - (\zeta_T + \delta_T + \mu_H) I_{HT},\\
I'_{RT} &= (1-\pi_1)\lambda_T E_{HT} + \zeta_{S2} I_{RS2} - \lambda_J I_{RT} - (\zeta_R + \delta_R + \mu_H) I_{RT},\\
T'_{HT} &= \zeta_T I_{HT} + \zeta_R I_{RT} - \xi\lambda_T T_{HT} - \lambda_J T_{HT} - \mu_H T_{HT},\\
E'_{HS} &= \lambda_J(S_H + T_{HT} + \psi T_{HS}) + \zeta_{T1} I_{ST} + \zeta_{R1} I_{RS1} - \eta_1\lambda_T E_{HS}\\
&\quad - (\alpha_1 + \mu_H) E_{HS},\\
I'_{HS} &= \alpha_1 E_{HS} + \zeta_{T2} I_{RS2} + \zeta_{T3} I_{TS} - \eta_2\lambda_T I_{HS} - (\zeta_S + \delta_S + \mu_H) I_{HS},\\
T'_{HS} &= \zeta_S I_{HS} - \lambda_T T_{HS} - \psi\lambda_J T_{HS} - \mu_H T_{HS},\\
E'_{TS} &= (1-m)\eta_1\lambda_T E_{HS} + \lambda_J E_{HT} - (1-\pi_2)\lambda_T E_{TS} - (\alpha_2 + \kappa_2 + \mu_H) E_{TS},\\
I'_{ST} &= m\eta_1\lambda_T E_{HS} + \lambda_J I_{HT} + \lambda_J I_{RT} + \kappa_2 E_{TS} - (\zeta_{T1} + \sigma + \chi_1\delta_T + \mu_H) I_{ST},\\
I'_{RS1} &= (1-\pi_2)\lambda_T E_{TS} - (\alpha_3 + \zeta_{R1} + \tau_1\delta_R + \mu_H) I_{RS1},\\
E'_{ST} &= (1-f)\eta_2\lambda_T I_{HS} + \alpha_2 E_{TS} - (1-\pi_3)\lambda_T E_{ST}\\
&\quad - (\zeta_{S1} + \kappa_3 + \upsilon_1\delta_S + \mu_H) E_{ST},\\
I'_{RS2} &= (1-\pi_3)\lambda_T E_{ST} + \alpha_3 I_{RS1} - (\zeta_{T2} + \zeta_{S2} + \tau_2\delta_R + \upsilon_2\delta_S + \mu_H) I_{RS2},\\
I'_{TS} &= f\eta_2\lambda_T I_{HS} + \kappa_3 E_{ST} + \sigma I_{ST} - (\zeta_{T3} + \zeta_{S3} + \chi_2\delta_T + \upsilon_3\delta_S + \mu_H) I_{TS},\\
L' &= N_e\gamma(I_{HS} + E_{ST} + I_{RS2} + I_{TS}) - \mu_L L,\\
S'_S &= \Lambda_S - \lambda_L S_S - \mu_S S_S,\\
I'_S &= \lambda_L S_S - \mu_S I_S,\\
J' &= \phi I_S - \mu_J J.
\end{aligned}
\tag{2.3}
$$

Table 1: Description of parameters of model (2.3)

Parameter	Description
Λ_H	Recruitment rate for humans
μ_H	Natural human mortality rate
β_T	Tuberculosis transmission rate
ξ	Lowered rate of reinfection with TB after recovery from a previous infection
f, m, p	Fraction of fast progressors to TB
π_1, π_2, π_3	Exogenous re-infection rates
$\kappa_1, \kappa_2, \kappa_3$	Endogenous reactivation rates
$\zeta_T, \zeta_{T1}, \zeta_{T2}, \zeta_{T3}, \zeta_R, \zeta_{R1}$	Treatment rates for TB
δ_T, δ_R	TB-induced human death rates
ψ	Reduced rate of infection with schistosomiasis after recovery from a previous infection
α_1	Progression rate from latent to active schistosomiasis infection
α_2	Rate of progression from exposed to both TB/schistosomiasis to exposed to TB/active schistosomiasis
α_3	Rate of progression from exogenously re-infected with TB/exposed to schistosomiasis to exogenously re-infected with TB/active schistosomiasis
$\zeta_S, \zeta_{S1}, \zeta_{S2}, \zeta_{S3}$	Treatment rates for schistosomiasis
δ_S	Schistosomiasis-induced human death rate
σ	Rate of progression from active TB/exposed to schistosomiasis to active TB/active schistosomiasis
χ_1, χ_2	Adjustment parameters for increased TB mortality due to co-infection
η_1, η_2	Adjustment parameters for the increased susceptibility to TB of humans with latent and active schistosomiasis
Θ_{RT}	Adjustment parameters which account for the decreased probability of transmission of TB by humans exogenously re-infected with TB
$\Theta_{RS1}, \Theta_{RS2}$	Adjustment parameters for the increased probability of transmission of TB by humans exogenously re-infected with TB, and exposed to/active schistosomiasis, respectively
Π_1, Π_2	Adjustment parameters for the increased probability of infectiousness of humans with active TB and latent/active schistosomiasis respectively
τ_1, τ_2	Adjustment parameters for increased TB mortality as a result of exogenous re-infection due to co-infection
v_1, v_2, v_3	Adjustment parameters which account for schistosomiasis-induced deaths
Λ_S	Snail population recruitment rate
μ_S	Mortality rate for snails
ϵ	Growth velocity limitation
L_0	Miracidia saturation constant
β_L	Infection rate of miracidia
N_e	Human-released egg count
γ	Success rate at which eggs transform into miracidia
μ_L	Mortality rate of miracidia
ϕ	Production rate of cercariae
J_0	Cercarial saturation constant
β_J	Infection rate of cercariae
μ_J	Mortality rate of cercariae

where the following lists the infection forces associated with tuberculosis (TB), schistosomiasis (which results from cercariae penetration), and snail infection by miracidia, respectively:

$$\lambda_T = \frac{\beta_T(I_{HT} + \Theta_{RT}I_{RT} + \Theta_{RS1}I_{RS1} + \Theta_{RS2}I_{RS2} + \Pi_1 I_{ST} + \Pi_2 I_{TS})}{N_H}, \quad (2.4)$$

$$\lambda_J = \frac{\beta_J J}{J_0 + \epsilon J}, \quad (2.5)$$

$$\lambda_L = \frac{\beta_L L}{L_0 + \epsilon L}. \quad (2.6)$$

2.1 Basic properties of the TB-schistosomiasis model (2.3)

The basic dynamical properties of the model (2.3) will now be investigated. Specifically, we establish the following positivity and boundedness results.

2.1.1 Positivity and boundedness of solutions

For the TB-schistosomiasis co-infection model (2.3) to be epidemiologically relevant, it is critical to demonstrate that every trajectory with positive inaugural data remains positive for all time and the biological feasible region will also remain positively-invariant for all time. Using a similar approach in [44, 52], the following results can be established.

Theorem 2.1. *Permit the inaugural data for the model for TB-schistosomiasis co-infection (2.3) to be given as* $S_H(0) > 0$, $E_{HT}(0) > 0$, $I_{HT}(0) > 0$, $I_{RT}(0) > 0$, $T_{HT}(0) > 0$, $E_{HS}(0) > 0$, $I_{HS}(0) > 0$, $T_{HS}(0) > 0$, $E_{TS}(0) > 0$, $I_{ST}(0) > 0$, $I_{RS1}(0) > 0$, $E_{ST}(0) > 0$, $I_{RS2}(0) > 0$, $I_{TS}(0) > 0$, $L(0) > 0$, $S_S(0) > 0$, $I_S(0) > 0$ *and* $J(0) > 0$. *Then the orbits* $\big(S_H(t)$, $E_{HT}(t)$, $I_{HT}(t)$, $I_{RT}(t)$, $T_{HT}(t)$, $E_{HS}(t)$, $I_{HS}(t)$, $T_{HS}(t)$, $E_{TS}(t)$, $I_{ST}(t)$, $I_{RS1}(t)$, $E_{ST}(t)$, $I_{RS2}(t)$, $I_{TS}(t)$, $L(t)$, $S_S(t)$, $I_S(t)$,

$J(t)\big)$ *of the model with positive initial conditions, will remain positive for all time* $t > 0$.

Proof:

Recall the premier equation of model (2.3), we have

$$\frac{dS_H(t)}{dt} = \Lambda_H - (\lambda_T + \lambda_J + \mu_H)S_H(t), \tag{2.7}$$

which is re-expressed as

$$\begin{aligned}\frac{d}{dt}\Big[S_H(t)\exp\Big\{\mu_H t + \int_0^t (\lambda_T(\tau) + \lambda_J(\tau))d\tau\Big\}\Big] \\ \geq \Lambda_H \exp\Big\{\mu_H t + \int_0^t (\lambda_T(\tau) + \lambda_J(\tau))d\tau\Big\}.\end{aligned} \tag{2.8}$$

Hence, proceeding to integrate (2.8) with regards to $t \in [0, t_1]$, we have

$$\begin{aligned}S_H(t_1)\exp\Big\{\mu t_1 + \int_0^{t_1} (\lambda_T(\tau) + \lambda_J(\tau))d\tau\Big\} - S_H(0) \\ \geq \int_0^{t_1} \Lambda_H\Big[\exp\Big\{\mu_H y + \int_0^y (\lambda_T(\tau) + \lambda_J(\tau))d\tau\Big\}\Big]dy,\end{aligned} \tag{2.9}$$

So that,

$$\begin{aligned}S_H(t_1) \geq S_H(0)\exp\Big[-\mu_H t_1 - \int_0^{t_1} (\lambda_T(\tau) + \lambda_J(\tau))d\tau\Big] \\ + \Big[\exp\Big\{-\mu_H t_1 - \int_0^{t_1} (\lambda_T(\tau) + \lambda_J(\tau))d\tau\Big\}\Big] \\ \times \int_0^{t_1} \Lambda_H\Big[\exp\Big\{\mu_H y + \int_0^y (\lambda_T(\tau) + \lambda_J(\tau))d\tau\Big\}\Big]dy > 0.\end{aligned} \tag{2.10}$$

Therefore $S_H(t) > 0,\ \forall\ t > 0$.

Equivalently, recalling equations two to the eighteen of model (2.3), we have that $E_{HT}(t) > 0,\ I_{HT}(t) > 0,\ I_{RT}(t) > 0,\ T_{HT}(t) > 0,\ E_{HS}(t) > 0,\ I_{HS}(t) > 0,\ T_{HS}(t) > 0,\ E_{TS}(t) > 0,\ I_{ST}(t) > 0,\ I_{RS1}(t) > 0,\ E_{ST}(t) > 0,\ I_{RS2}(t) > 0,\ I_{TS}(t) > 0,\ L(t) > 0,\ S_S(t) > 0,\ I_S(t) > 0$ and $J(t) > 0,\ \forall\ t > 0$.

Theorem 2.2. *Permit* $\big(S_H(t),\ E_{HT}(t),\ I_{HT}(t),\ I_{RT}(t),\ T_{HT}(t),\ I_{HS}(t),\ T_{HS}(t),\ E_{TS}(t),\ I_{ST}(t),\ I_{RS1}(t),\ E_{ST}(t),\ I_{RS2}(t),\ I_{TS}(t),\ L(t),\ S_S(t),\ I_S(t),\ J(t)\big)$ *to be trajectories of the system* (2.3) *along side basic circumstances and the biological reasonable region given by the set*

$$\mathcal{D} = \mathcal{D}_H \times \mathcal{D}_L \times \mathcal{D}_S \times \mathcal{D}_J \subset \mathbb{R}_+^{14} \times \mathbb{R}_+^1 \times \mathbb{R}_+^2 \times \mathbb{R}_+^1 \subset \mathbb{R}_+^{18}$$

where:
$\mathcal{D}_H = \{(S_H,\ E_{HT},\ I_{HT},\ I_{RT},\ T_{HT},\ E_{HS},\ I_{HS},\ T_{HS}, E_{TS},\ I_{ST},\ I_{RS1},\ E_{ST},\ I_{RS2},\ I_{TS}) \in \mathbb{R}_+^{14} : N_H \leq \frac{\Lambda_H}{\mu_H}\}$
$\mathcal{D}_L = \{L \in \mathbb{R}_+^1 : L \leq \frac{N_e\gamma\Lambda_H}{\mu_L\mu_H}\}$
$\mathcal{D}_S = \{(S_S, I_S) \in \mathbb{R}_+^2 : N_S \leq \frac{\Lambda_S}{\mu_S}\}$
$\mathcal{D}_J = \{J \in \mathbb{R}_+^1 : J \leq \frac{\phi\Lambda_S}{\mu_J\mu_S}\}$
is invariant positively and attracts every positive trajectory of the model (2.3).

Proof:
Summing up the right side of the vector field for the entire human populace in both patches in (2.3), yields

$$\frac{dN_H}{dt} = \Lambda_H - \mu_H N - (\delta_T I_{HT} + \delta_R I_{RT} + \delta_S I_{HS} + \chi_1\delta_T I_{ST} + \tau_1\delta_R I_{RS1} + v_1\delta_S E_{ST} + (\tau_2\delta_R + v_2\delta_S)I_{RS2} + (\chi_2\delta_T + v_3\delta_S)I_{TS}. \quad (2.11)$$

From (2.11), it ensues that $\frac{dN_H}{dt} \leq \Lambda_H - \mu_H N_H$. Hence, $\frac{dN_H}{dt} \leq 0$ if $N_H(t) \geq \frac{\Lambda_H}{\mu_H}$. Utilizing [25] comparison theorem, we show that

$$N_H(t) \leq N_H(0)e^{-\mu_H t} + \frac{\Lambda_H}{\mu_H}(1 - e^{-\mu_H t}) \quad (2.12)$$

Specifically, on the condition that $N_H(0) \leq \frac{\Lambda_H}{\mu_H}$, then $N_H(t) \leq \frac{\Lambda_H}{\mu_H}$ for every $t > 0$. Thus, the set $\mathcal{D}_H$ is invariant positively. Moreover, if $N_H(0) > \frac{\Lambda_H}{\mu_H}$, then one or the other flows invade the set $\mathcal{D}_H$ in finite time or $N_H(t)$ asymptotically advances in the direction of $\frac{\Lambda_H}{\mu_H}$ as $t \to \infty$. Thus, the set $\mathcal{D}_H$ attracts all trajectories in $\mathbb{R}_+^{16}$.

From (2.11), it ensues that $\frac{dN_H}{dt} \leq \Lambda_H - \mu_H N_H$. Hence, $\frac{dN_H}{dt} \leq 0$ if $N_H(t) \geq$

$\frac{\Lambda_H}{\mu_H}$. Utilizing [25] comparison theorem, we show that

$$N_H(t) \leq N_H(0)e^{-\mu_H t} + \frac{\Lambda_H}{\mu_H}(1 - e^{-\mu_H t}) \tag{2.13}$$

Specifically, if $N_H(0) \leq \frac{\Lambda_H}{\mu_H}$, then $N_H(t) \leq \frac{\Lambda_H}{\mu_H}$ for all $t > 0$. Therefore, the set $\mathcal{D}_H$ is invariant in a positive way. Moreover, if $N_H(0) > \frac{\Lambda_H}{\mu_H}$, then one of the two happens: the flows penetrate the set $\mathcal{D}_H$ in fixed time or $N_H(t)$ asymptotically advances in the direction of $\frac{\Lambda_H}{\mu_H}$ as $t \to \infty$. Hence, the set $\mathcal{D}_H$ serves as an attractor for every trajectory in $\mathbb{R}^{16}_+$.

For the concentration of the miracidia, from (2.3), we have

$$\frac{dL}{dt} = N_e\gamma(I_{HS} + E_{ST} + I_{RS2} + I_{TS}) - \mu_L L. \tag{2.14}$$

From (2.14), which ensues that $\frac{dL}{dt} \leq \frac{N_e\gamma\Lambda_H}{\mu_H} - \mu_L L$ since $N_H = S_H + E_{HT} + I_{HT} + I_{RT} + T_{HT} + E_{HS} + I_{HS} + T_{HS} + E_{TS} + I_{ST} + I_{RS1} + E_{ST} + I_{RS2} + I_{TS} \leq \frac{\Lambda_H}{\mu_H} \Longrightarrow I_{HS} + E_{TS} + I_{RS2} + I_{TS} \leq \frac{\Lambda_H}{\mu_H}$. Thus, $\frac{dL}{dt} \leq 0$ if $L(t) \geq \frac{N_e\gamma\Lambda_H}{\mu_L\mu_H}$. Utilizing [25] comparison theorem, we reveal that $L(t) \leq L(0)e^{-\mu_L t} + \frac{N_e\gamma\Lambda_H}{\mu_L\mu_H}(1 - e^{-\mu_L t})$.

Specifically, if $L(0) \leq \frac{N_e\gamma\Lambda_H}{\mu_L\mu_H}$, then $L(t) \leq \frac{N_e\gamma\Lambda_H}{\mu_L\mu_H}$ for all $t > 0$. Hence, the set $\mathcal{D}_L$ is invariant in a positive way. Moreover, if $L(0) > \frac{N_e\gamma\Lambda_H}{\mu_L\mu_H}$, thereupon one of the two happens: the orbits penetrate the set $\mathcal{D}_L$ in fixed time or $L(t)$ asymptotically advances in the direction of $\frac{N_e\gamma\Lambda_H}{\mu_L\mu_H}$ as $t \to \infty$. Hence, the set $\mathcal{D}_L$ serves as an attractor for every solution in $\mathbb{R}^1_+$.

For the entire snail populace, we add up the right hand side of the vector field of the population of snails in (2.3), which gives

$$\frac{dN_S}{dt} = \Lambda_S - \mu_S N_S. \tag{2.15}$$

From (2.15), it ensues that $\frac{dN_S}{dt} \leq 0$ if $N_S(t) \geq \frac{\Lambda_S}{\mu_S}$. It implies that $N_S(t) = N_S(0)e^{-\mu_S t} + \frac{\Lambda_S}{\mu_S}(1 - e^{-\mu_S t})$. Then the $\limsup_{t\to\infty} N_S(t) = \frac{\Lambda_S}{\mu_S}$.

In particular, if $N_S(0) \leq \frac{\Lambda_S}{\mu_S}$, then $N_S(t) \leq \frac{\Lambda_S}{\mu_S}$ for all $t > 0$. Hence, the set $\mathcal{D}_S$ is invariant in a positive way. Moreover, if $N_S(0) > \frac{\Lambda_S}{\mu_S}$, thereupon one of the two happens: the flows enter the set $\mathcal{D}_S$ in fixed time or $N_S(t)$ asymptotically advances in the direction $\frac{\Lambda_S}{\mu_S}$ as $t \to \infty$. Hence, the set $\mathcal{D}_S$ attracts every trajectory in $\mathbb{R}^2_+$.

For the cercariae concentration, we recall the right hand side of the vector field J in (2.3), we obtain

$$\frac{dJ}{dt} = \phi I_S - \mu_J J. \tag{2.16}$$

From (2.16), $\frac{dJ}{dt} = \phi I_S - \mu_J J$ which follows that $\frac{dJ}{dt} \leq \frac{\phi\Lambda_S}{\mu_S} - \mu_J J$ since $N_S = S_S + I_S \leq \frac{\Lambda_S}{\mu_S} \Longrightarrow I_S \leq \frac{\Lambda_S}{\mu_S}$. Therefore, $\frac{dJ}{dt} \leq 0$ if $J(t) \geq \frac{\phi\Lambda_S}{\mu_J\mu_S}$. Utilizing [25] standard comparison theorem, we reveal that $J(t) \leq J(0)e^{-\mu_J t} + \frac{\phi\Lambda_S}{\mu_J\mu_S}(1 - e^{-\mu_J t})$. Specifically, if $J(0) \leq \frac{\phi\Lambda_S}{\mu_J\mu_S}$, then $J(t) \leq \frac{\phi\Lambda_S}{\mu_J\mu_S}$ for all $t > 0$. Hence, the set $\mathcal{D}_J$ is invariant in a positive way. Moreover, if $J(0) > \frac{\phi\Lambda_S}{\mu_J\mu_S}$, thereupon one of the two happens: the flows enter the set $\mathcal{D}_J$ in fixed time or $J(t)$ asymptotically advances in the direction of $\frac{\phi\Lambda_S}{\mu_J\mu_S}$ as $t \to \infty$. Thus, the set $\mathcal{D}_J$ attracts every trajectory in $\mathbb{R}^1_+$.

From the above, we have shown that $\mathcal{D}_H, \mathcal{D}_L, \mathcal{D}_S$ and $\mathcal{D}_J$ are invariant in a positive way and since $\mathcal{D} = \mathcal{D}_H \times \mathcal{D}_L \times \mathcal{D}_S \times \mathcal{D}_J$, it implies that the set $\mathcal{D}$ is invariant in a positive way and an attractor, so that no trajectory escapes through any boundary of $\mathcal{D}$.

$$\mathcal{D} = \begin{cases} (S_H, E_{HT}, I_{HT}, I_{RT}, T_{HT}, E_{HS}, I_{HS}, T_{HS}, E_{TS}, I_{ST}, I_{RS1}, E_{ST}, I_{RS2}, \\ I_{TS}) \in \mathbb{R}^{14}_+ : N_H \leq \frac{\Lambda_H}{\mu_H} \\ L \in \mathbb{R}^1_+ : L \leq \frac{N_e\gamma\Lambda_H}{\mu_L\mu_H} \\ (S_S, I_S) \in \mathbb{R}^2_+ : N_S \leq \frac{\Lambda_S}{\mu_S} \\ J \in \mathbb{R}^1_+ : J \leq \frac{\phi\Lambda_S}{\mu_J\mu_S} \end{cases} \tag{2.17}$$

Thus, analyzing the flow patterns produced by the model (2.3) in $\mathcal{D}$ suffices.

We declare, therefore, that the model (2.3) is well-posed mathematically and epidemiologically.

3 Mathematical Analysis of the Model

We proceed with the analysis of the full co-infection model 2.3.

3.1 Model (2.3)'s local asymptotic stability of the DFE

The model system (2.3) possesses a disease-free equilibrium, that is, the DFE, represented by

$$\begin{aligned}\mathcal{E}_0 =&(S_H^*, E_{HT}^*, I_{HT}^*, I_{RT}^*, T_{HT}^*, E_{HS}^*, I_{HS}^*, T_{HS}^*, E_{TS}^*, I_{ST}^*, I_{RS1}^*, E_{ST}^*, I_{RS2}^*, I_{TS}^*,\\ & L^*, S_S^*, I_S^*, J^*)\\ =&(\frac{\Lambda_H}{\mu_H}, 0,0,0,0,0,0,0,0,0,0,0,0,0,0,0,\frac{\Lambda_S}{\mu_S}, 0, 0)\end{aligned}$$

It can be shown, employing the next-generation operator method [56](van den Driessche and Watmough, 2002), that the corresponding effective reproduction number of the model (2.3), $\mathcal{R}_{TS}$, is represented by

$$\mathcal{R}_{TS} = max\left\{\mathcal{R}_{HT}, \mathcal{R}_{HS}\right\} \tag{3.1}$$

where

$$\mathcal{R}_{HT} = \frac{\beta_T((1-p)\kappa_1 + p(\kappa_1+\mu_H))}{(\kappa_1+\mu_H)(\zeta_T+\delta_T+\mu_H)},$$

$$\mathcal{R}_{HS} = \sqrt{\frac{\alpha_1\beta_J\beta_L\Lambda_H\Lambda_S N_e\gamma\varphi}{J_0L_0\mu_H\mu_J\mu_L\mu_S^2(\alpha_1+\mu_H)(\zeta_S+\delta_S+\mu_H)}}$$

are the respective *effective reproduction number* for TB-only and schistosomiasis-only disease transmission dynamics in (2.3). Utilizing Theorem 2 in [56], we establish the following conclusion:

Lemma 3.1. *The infection-free equilibrium (DFE), $\mathcal{E}_0$, is locally asymptotically stable (LAS) in $\mathcal{D}$ on the grounds that $\mathcal{R}_{TS} < 1$ and unstable given that $\mathcal{R}_{TS} > 1$.*

The threshold number, $\mathcal{R}_{TS}$, is a calibration of the mean number of secondary cases created by a single infected human individual in a totally exposed populace [23]. This implies that a little influx of infected humans would not generate large outbreaks if $\mathcal{R}_{TS} < 1$, and the epidemic will prevail in the populace if $\mathcal{R}_{TS} > 1$.

3.2 Backward bifurcation analysis

Due to the large number of variables and parameters of model (2.3), it is mathematically intractable to show the existence of the unique endemic equilibrium point (EEP). However, we proceed to analyse model (2.3) for the cause(s) of the existence of the backward bifurcation phenomenon. Adopting the method in [9], we claim the following result.

Theorem 3.1. *If $\mathcal{R}_{TS} < 1$ and the bifurcation coefficients a and b are both positive (i.e., $a > 0$, $b > 0$), then (2.3) exhibits a backward bifurcation at $\mathcal{R}_{TS} = 1$, otherwise the equation exhibits a forward bifurcation.*

Proof: The presence of backward bifurcation is explored utilizing the *Center Manifold Theory* as espoused [9].

Let $S_H = x_1$, $E_{HT} = x_2$, $I_{HT} = x_3$, $I_{RT} = x_4$, $T_{HT} = x_5$, $E_{HS} = x_6$, $I_{HS} = x_7$, $T_{HS} = x_8$, $E_{TS} = x_9$, $I_{ST} = x_{10}$, $I_{RS1} = x_{11}$, $E_{ST} = x_{12}$, $1_{RS2} = x_{13}$, $I_{TS} = x_{14}$, $L = x_{15}$, $S_S = x_{16}$, $I_S = x_{17}$ and $J = x_{18}$, so that $N_H = \sum_{i=1}^{14} x_i$; hence the model (2.3) is re-written in the form

$$
\begin{aligned}
\dot{x}_1 &\equiv f_1 = \Lambda_H - \lambda_T x_1 - \lambda_J x_1 - \mu_H x_1,\\
\dot{x}_2 &\equiv f_2 = (1-p)\lambda_T(x_1 + \xi x_5 + x_8) + \zeta_{S1}x_{12} - (1-\pi_1)\lambda_T x_2 - \lambda_J x_2 - M_1 x_2,\\
\dot{x}_3 &\equiv f_3 = p\lambda_T(x_1 + \xi x_5 + x_8) + \kappa_1 x_2 + \zeta_{S3}x_{14} - \lambda_J x_3 - M_2 x_3,\\
\dot{x}_4 &\equiv f_4 = (1-\pi_1)\lambda_T x_2 + \zeta_{S2}x_{13} - \lambda_J x_4 - M_3 x_4,\\
\dot{x}_5 &\equiv f_5 = \zeta_T x_3 + \zeta_R x_4 - \xi\lambda_T x_5 - \lambda_J x_5 - \mu_H x_5,\\
\dot{x}_6 &\equiv f_6 = \lambda_J(x_1 + x_5 + \psi x_8) + \zeta_{T1}x_{10} + \zeta_{R1}x_{11} - \eta_1\lambda_T x_6 - M_4 x_6,\\
\dot{x}_7 &\equiv f_7 = \alpha_1 x_6 + \zeta_{T2}x_{13} + \zeta_{T3}x_{14} - \eta_2\lambda_T x_7 - M_5 x_7,\\
\dot{x}_8 &\equiv f_8 = \zeta_S x_7 - \lambda_T x_8 - \psi\lambda_J x_8 - \mu_H x_8,\\
\dot{x}_9 &\equiv f_9 = (1-m)\eta_1\lambda_T x_6 + \lambda_J x_2 - (1-\pi_2)\lambda_T x_9 - M_6 x_9,\\
\dot{x}_{10} &\equiv f_{10} = m\eta_1\lambda_T x_6 + \lambda_J x_3 + \lambda_J x_4 + \kappa_2 x_9 - M_7 x_{10},\\
\dot{x}_{11} &\equiv f_{11} = (1-\pi_2)\lambda_T x_9 - M_8 x_{11},\\
\dot{x}_{12} &\equiv f_{12} = (1-f)\eta_2\lambda_T x_7 + \alpha_2 x_9 - (1-\pi_3)\lambda_T x_{12} - M_9 x_{12},\\
\dot{x}_{13} &\equiv f_{13} = (1-\pi_3)\lambda_T x_{12} + \alpha_3 x_{11} - M_{10} x_{13},\\
\dot{x}_{14} &\equiv f_{14} = f\eta_2\lambda_T x_7 + \kappa_3 x_{12} + \sigma x_{10} - M_{11} x_{14},\\
\dot{x}_{15} &\equiv f_{15} = N_e\gamma(x_7 + x_{12} + x_{13} + x_{14}) - \mu_L x_{15},\\
\dot{x}_{16} &\equiv f_{16} = \Lambda_S - \lambda_L x_{16} - \mu_S x_{16},\\
\dot{x}_{17} &\equiv f_{17} = \lambda_L x_{16} - \mu_S x_{17},\\
\dot{x}_{18} &\equiv f_{18} = \phi x_{17} - \mu_J x_{18}.
\end{aligned}
\tag{3.2}
$$

Then the forces of infection for our model (3.2) become:

$$
\lambda_T = \frac{\beta_T(x_3 + \Theta_{RT}x_4 + \Theta_{RS1}x_{11} + \Theta_{RS2}x_{13} + \Pi_1 x_{10} + \Pi_2 x_{14})}{\sum_{i=1}^{14} x_i},
$$

$$
\lambda_J = \frac{\beta_J x_{18}}{J_0 + \epsilon x_{18}}, \quad \lambda_L = \frac{\beta_L x_{15}}{L_0 + \epsilon x_{15}}.
$$

where $M_1 = \kappa_1 + \mu_H$, $M_2 = \zeta_T + \delta_T + \mu_H$, $M_3 = \zeta_R + \delta_R + \mu_H$, $M_4 = \alpha_1 + \mu_H$, $M_5 = \zeta_S + \delta_S + \mu_H$, $M_6 = \alpha_2 + \kappa_2 + \mu_H$,

$M_7 = \zeta_{T1} + \sigma + \chi_1\delta_T + \mu_H$, $M_8 = \alpha_3 + \zeta_{R1} + \tau_1\delta_R + \mu_H$,
$M_9 = \zeta_{S1} + \kappa_3 + v_1\delta_S + \mu_H$, $M_{10} = \zeta_{T2} + \zeta_{S2} + \tau_2\delta_R + v_2\delta_S + \mu_H$, and
$M_{11} = \zeta_{T3} + \zeta_{S3} + \chi_2\delta_T + v_3\delta_S + \mu_H$.

Consider the case with $\beta_T = \beta_T^*$ and $\beta_J = \beta_J^*$ as bifurcation parameters. Figuring out $\beta_T = \beta_T^*$ and $\beta_J = \beta_J^*$ from $\mathcal{R}_{TS} = 1$ yields

$$\begin{aligned}\beta_T = \beta_T^* &= \frac{(\kappa_1 + \mu_H)(\zeta_T + \delta_T + \mu_H)}{[(1-p)\kappa_1 + p(\kappa_1 + \mu_H)]},\\ \beta_J = \beta_J^* &= \frac{J_0 L_0 \mu_H \mu_J \mu_L \mu_S^2 (\alpha_1 + \mu_H)(\zeta_S + \delta_S + \mu_H)}{\alpha_1 \beta_L \Lambda_H \Lambda_S N_e \gamma \phi}\end{aligned} \tag{3.3}$$

The system (3.2) possesses a Jacobian at the infection-free equilibrium with $\beta_T = \beta_T^*$, is represented by:

$$J_{\beta_T^*} = J(\mathcal{E}_0)|_{\beta_T^*} = \begin{pmatrix} P_{11} & P_{12} \\ P_{21} & P_{22} \end{pmatrix}, \tag{3.4}$$

where

$$P_{11} = \begin{pmatrix} -\mu_H & 0 & -\beta_T^* & -\beta_T^*\Theta_{RT} & 0 & 0 & 0 & 0 & 0 \\ 0 & -M_1 & (1-p)\beta_T^* & (1-p)\beta_T^*\Theta_{RT} & 0 & 0 & 0 & 0 & 0 \\ 0 & \kappa_1 & p\beta_T^* - M_2 & p\beta_T^*\Theta_{RT} & 0 & 0 & 0 & 0 & 0 \\ 0 & 0 & 0 & -M_3 & 0 & 0 & 0 & 0 & 0 \\ 0 & 0 & \zeta_T & \zeta_R & -\mu_H & 0 & 0 & 0 & 0 \\ 0 & 0 & 0 & 0 & 0 & -M_4 & 0 & 0 & 0 \\ 0 & 0 & 0 & 0 & 0 & \alpha_1 & -M_5 & 0 & 0 \\ 0 & 0 & 0 & 0 & 0 & 0 & \zeta_S & -\mu_H & 0 \\ 0 & 0 & 0 & 0 & 0 & 0 & 0 & 0 & -M_6 \end{pmatrix}, \tag{3.5}$$

$$P_{12} = \begin{pmatrix} -\beta_T^*\Pi_1 & -\beta_T^*\Theta_{RS1} & 0 & -\beta_T^*\Theta_{RS2} & \beta_T^*\Pi_2 & 0 & 0 & 0 & -\beta_J A_* \\ (1-p)\beta_T^*\Pi_1 & (1-p)\beta_T^*\Theta_{RS1} & \zeta_{S1} & (1-p)\beta_T^*\Theta_{RS2} & (1-p)\beta_T^*\Pi_2 & 0 & 0 & 0 & 0 \\ p\beta_T^*\Pi_1 & p\beta_T^*\Theta_{RS1} & 0 & p\beta_T^*\Theta_{RS2} & p)\beta_T^*\Pi_2 + \zeta_{S3} & 0 & 0 & 0 & 0 \\ 0 & 0 & 0 & \zeta_{S2} & 0 & 0 & 0 & 0 & 0 \\ 0 & 0 & 0 & 0 & 0 & 0 & 0 & 0 & 0 \\ \zeta_{T1} & \zeta_{R1} & 0 & 0 & 0 & 0 & 0 & 0 & \beta_J A_* \\ 0 & 0 & 0 & \zeta_{T2} & \zeta_{T3} & 0 & 0 & 0 & 0 \\ 0 & 0 & 0 & 0 & 0 & 0 & 0 & 0 & 0 \\ 0 & 0 & 0 & 0 & 0 & 0 & 0 & 0 & 0 \end{pmatrix}, \tag{3.6}$$

$$P_{21} = \begin{pmatrix} 0 & 0 & 0 & 0 & 0 & 0 & 0 & 0 & \kappa_2 \\ 0 & 0 & 0 & 0 & 0 & 0 & 0 & 0 & 0 \\ 0 & 0 & 0 & 0 & 0 & 0 & 0 & 0 & \alpha_2 \\ 0 & 0 & 0 & 0 & 0 & 0 & 0 & 0 & 0 \\ 0 & 0 & 0 & 0 & 0 & 0 & 0 & 0 & 0 \\ 0 & 0 & 0 & 0 & 0 & 0 & N_e\gamma & 0 & 0 \\ 0 & 0 & 0 & 0 & 0 & 0 & 0 & 0 & 0 \\ 0 & 0 & 0 & 0 & 0 & 0 & 0 & 0 & 0 \\ 0 & 0 & 0 & 0 & 0 & 0 & 0 & 0 & 0 \end{pmatrix}, \tag{3.7}$$

$$P_{22} = \begin{pmatrix} -M_7 & 0 & 0 & 0 & 0 & 0 & 0 & 0 & 0 \\ 0 & -M_8 & 0 & 0 & 0 & 0 & 0 & 0 & 0 \\ 0 & 0 & -M_9 & 0 & 0 & 0 & 0 & 0 & 0 \\ 0 & \alpha_3 & 0 & -M_{10} & 0 & 0 & 0 & 0 & 0 \\ \sigma & 0 & \kappa_3 & 0 & -M_{11} & 0 & 0 & 0 & 0 \\ 0 & 0 & N_e\gamma & N_e\gamma & N_e\gamma & -\mu_L & 0 & 0 & 0 \\ 0 & 0 & 0 & 0 & 0 & -\beta_L A_{**} & -\mu_S & 0 & 0 \\ 0 & 0 & 0 & 0 & 0 & \beta_L A_{**} & 0 & -\mu_S & 0 \\ 0 & 0 & 0 & 0 & 0 & 0 & 0 & \phi & -\mu_J \end{pmatrix}. \tag{3.8}$$

and

$$A_* = \frac{\Lambda_H}{J_0\mu_H}, \qquad A_{**} = \frac{\Lambda_S}{L_0\mu_S}, \tag{3.9}$$

Consider the case when $\mathcal{R}_{TS} = 1$. We assume that the *maximum* of

$$\mathcal{R}_{TS} = max\left\{\mathcal{R}_{HT}, \mathcal{R}_{HS}\right\} = \mathcal{R}_{HT}. \tag{3.10}$$

Figuring out $\beta_T = \beta_T^*$ from $\mathcal{R}_{HT} = 1$ gives

$$\beta_T = \beta_T^* = \frac{(\kappa_1 + \mu_H)(\zeta_T + \delta_T + \mu_H)}{[(1-p)\kappa_1 + p(\kappa_1 + \mu_H)]} \tag{3.11}$$

Matrix $J_{\beta_T^*}$ possesses a right eigenvector given by $\mathbf{w} = (w_1, w_2, ..., w_{18})^T$, where

$$\begin{aligned}
&w_1 = -\frac{(\beta_T^* w_3 + \beta_J A_* w_{18})}{\mu_H}, w_2 = \frac{(1-p)\beta_T^*}{M_1(M_2 - p\beta_T^*)},\\
&w_3 = \frac{M_1}{(1-p)\kappa_1\beta_T^*}, w_4 = 0, w_5 = \frac{\zeta_T w_3}{\mu_H},\\
&w_6 = \frac{\beta_J A_* w_{18}}{M_4}, w_7 = \frac{\mu_J\mu_L\mu_S w_{18}}{\beta_L\phi N_e\gamma A_{**}}, w_8 = \frac{\zeta_S\mu_J\mu_L\mu_S w_{18}}{\beta_L\phi N_e\gamma A_{**}},\\
&w_9 = w_{10} = w_{11} = w_{12} = w_{13} = w_{14} = 0,\\
&w_{15} = \frac{\mu_J\mu_S w_{18}}{\beta_L\phi A_{**}}, w_{16} = -\frac{\mu_J w_{18}}{\phi}, w_{17} = \frac{\mu_J w_{18}}{\phi}, w_{18} = w_{18} > 0.
\end{aligned} \tag{3.12}$$

In addition, $J_{\beta_T^*}$ possesses a left eigenvector $\mathbf{v} = (\nu_1, \nu_2, ..., \nu_{18})$ fulfilling $\mathbf{v.w} = \mathbf{1}$, with

$$
\begin{aligned}
\nu_1 &= 0, \nu_2 = \frac{\kappa_1}{M_1(M_2 - p\beta_T^*)}, \nu_3 = \frac{M_1}{(1-p)\kappa_1\beta_T^*},\\
\nu_4 &= \frac{((1-p)\nu_2 + p\nu_3)\beta_T^*\Theta_{RT}}{M_3}, \nu_5 = 0, \nu_6 = \frac{\mu_J\nu_{18}}{\beta_J A_*},\\
\nu_7 &= \frac{\beta_L\varphi N_e\gamma A_{**}}{\mu_L\mu_S M_5}, \nu_8 = 0, \nu_9 = \frac{\kappa_2\nu_{10} + \alpha_2\nu_{12}}{M_6},\\
\nu_{10} &= \frac{((1-p)\nu_2 + p\nu_3)\beta_T^*\Pi_1 + \zeta_{T1}\nu_6 + \sigma\nu_{14}}{M_7},\\
\nu_{11} &= \frac{((1-p)\nu_2 + p\nu_3)\beta_T^*\Theta_{RS1} + \zeta_{R1}\nu_6 + \alpha_3\nu_{13}}{M_8},\\
\nu_{12} &= \frac{\zeta_{S1}\nu_2 + \kappa_3\nu_{14} + N_e\gamma\nu_{15}}{M_9},\\
\nu_{13} &= \frac{((1-p)\nu_2 + p\nu_3)\beta_T^*\Theta_{RS2} + \zeta_{S2}\nu_4 + \zeta_{T2}\nu_7 + N_e\gamma\nu_{15}}{M_{10}},\\
\nu_{14} &= \frac{((1-p)\nu_2 + p\nu_3)\beta_T^*\Pi_2 + \zeta_{S3}\nu_3 + \zeta_{T3}\nu_7 + N_e\gamma\nu_{15}}{M_{11}},\\
\nu_{15} &= \frac{\beta_L\phi A_{**}\nu_{18}}{\mu_L\mu_S}, \nu_{16} = 0, \nu_{17} = \frac{\phi\nu_{18}}{\mu_S}, \nu_{18} = \nu_{18} > 0.
\end{aligned}
\tag{3.13}
$$

We compute the connected non-zero partial derivatives of the right sides of the modified system (3.2), (appraised at the disease-free equilibrium with $\beta_T = \beta_T^*$) that the related bifurcation coefficients, a and b, are given by

$$
a = \sum_{k,i,j=1}^{n} v_k w_i w_j \frac{\partial^2 f_k}{\partial x_i \partial x_j}(0,0), \qquad \text{and} \qquad b = \sum_{k,i=1}^{n} v_k w_i \frac{\partial^2 f_k}{\partial x_i \partial \beta_T^*}(0,0), \tag{3.14}
$$

where

$$
\begin{aligned}
a =& \frac{2\beta_T^*}{x_1^*}\Big[\Big(\frac{((1-p)\nu_2+p\nu_3)w_2\beta_T^*\Theta_{RT}(1-\pi_1)}{M_3}+\eta_1((1-m)\nu_9w_6+m\nu_{10}w_6)\\
&+\eta_2((1-f)\nu_{12}w_7+f\nu_{14}w_7)\Big)w_3\Big]\\
&+\frac{2\beta_J^*}{J_0}\Big[\psi\nu_6w_8w_{18}\Big]\\
&+\frac{2\beta_J^*}{J_0}\Big[\Big(\nu_6\frac{\zeta_Tw_3}{\mu_H}+\nu_9\frac{(1-p)\beta_T^*}{M_1(M_2-p\beta_T^*)}\\
&\qquad+\Big(\frac{((1-p)\nu_2+p\nu_3)\beta_T^*\Pi_1+\zeta_{T1}\nu_6+\sigma\nu_{14}}{M_7}\Big)w_3\Big)w_{18}\Big]\\
&-\frac{2\beta_T^*}{x_1^*}\Big[\Big(\nu_2(((1-p)+(1-\pi_1))w_2+(1-p)(w_3+(1-\xi)w_5+w_6+w_7))\\
&+p\nu_3(w_2+w_3+(1-\xi)w_5+w_6+w_7)+\eta_1\nu_6w_6+\eta_2\nu_7w_7\Big)w_3\Big]\\
&-\frac{2\beta_J^*}{J_0}\Big[\Big(\nu_2w_2+\nu_3w_3+\frac{\nu_6}{J_0}\Big(\frac{\beta_T^*J_0w_3+\beta_J^*x_1^*w_{18}}{\mu_H}+\epsilon x_1^*w_{18}\Big)\Big)w_{18}\Big]\\
&-\frac{2\beta_L}{L_0}\Big[\Big(\frac{\epsilon\phi x_{16}^*w_{15}+L_0\mu_Jw_{18}}{L_0\phi}\Big)\nu_{17}w_{15}\Big]
\end{aligned}
\tag{3.15}
$$

and

$$
b=((1-p)\nu_2+p\nu_3)w_3>0. \tag{3.16}
$$

However, since our interest is in identifying the parameter(s), which is(are) responsible for causing the bifurcation coefficient, a, to be negative, i.e. $a<0$, it is worthy of note, at this juncture, that [34–40, 53] had established that the relative rate of infectiousness of exogenously re-infected humans (Θ_{RT}, in this case) as a source of backward bifurcation in TB transmission dynamics. Similarly, it has also been reported by [1, 51] that re-infection is a cause of the backward bifurcation phenomenon in schistosomiasis disease dynamics. A careful scrutiny of (3.15) shows that eliminating the rate of relative infectiousness of exogenously re-infected humans (Θ_{RT}) and the reduced rate of re-infection with schistosomiasis (ψ) by setting their respective values to zero (i.e., $\Theta_{RT}=\psi=0$), will not completely

yield the desired result of eliminating the backward bifurcation phenomenon in a TB-schistosomiasis co-infection model. Hence, there must be other parameters responsible for this dilemma. Further scrutiny identifies the relative rates at which humans with latent schistosomiasis (η_1) and active schistosomiasis (η_2) are infected with TB, respectively, the treatment rate for all individuals infectious with only TB (ζ_T), the fraction of individuals who experience fast progression to active TB (p), the adjustment parameter which accounts for the elevated probability of infectiousness of people with active TB and latent schistosomiasis (Π_1), the treatment rate of individuals with active TB exposed to schistosomiasis (ζ_{T1}) and the rate of progression to active TB/exposed to schistosomiasis to active TB/active schistosomiasis (σ), as being responsible for the non-elimination of the backward bifurcation phenomenon from the TB-schistosomiasis co-infection model (2.3).

Thus, this study has shown that the existence of the relative rate of infectiousness of exogenously re-infected humans (Θ_{RT}), the relative rates at which humans with latent schistosomiasis (η_1) and active schistosomiasis (η_2) are infected with TB, respectively and the reduced rate of re-infection with schistosomiasis (ψ), the fraction of individuals who experience fast progression to active TB (p), the adjustment parameter which accounts for the elevated probability of infectiousness of humans with active TB and latent schistosomiasis (Π_1), the treatment rate of individuals with active TB exposed to schistosomiasis (ζ_{T1}) and the rate of progression to active TB/exposed to schistosomiasis to active TB/active schistosomiasis (σ) induce backward bifurcation in the disease dynamics of TB in the presence of schistosomiasis. Thus, the effective reproduction number, $\mathcal{R}_{TS}$, less than one, becomes a necessary but not a satisfactory condition for the control of both diseases in the population.

3.3 Global asymptotic stability (GAS) of DFE

We go ahead to investigate the global asymptotic stability (GAS) of the DFE of a special case of (2.3) with negligible relative rate of infectiousness of exogenously re-infected humans ($\Theta_{RT} = 0$), the relative rates at which humans with latent schistosomiasis ($\eta_1 = 0$) and active schistosomiasis ($\eta_2 = 0$) are infected with TB, respectively and the reduced rate of re-infection with schistosomiasis ($\psi = 0$), the fraction of individuals who experience fast progression to active TB ($p = 1$), the adjustment parameter which accounts for the elevated probability of infectiousness of humans with active TB and latent schistosomiasis ($\Pi_1 = 0$), the treatment rate of individuals with active TB exposed to schistosomiasis ($\zeta_{T1} = 0$) and the rate of progression to active TB/exposed to schistosomiasis to active TB/active schistosomiasis ($\sigma = 0$) in the absence of treatment for infected cases of TB and schistosomiasis, respectively. This leads to the elimination of the following human sub-populations: individuals exogenously re-infected with TB ($I_{RT} = 0$), individuals treated for TB ($T_{HT} = 0$), individuals treated for schistosomiasis ($T_{HS} = 0$), individuals exogenously re-infected with TB and exposed to schistosomiasis ($I_{RS1} = 0$), and individuals exogenously re-infected with TB and active schistosomiasis ($I_{RS2} = 0$). Using the idea in [36], we claim the following result.

Theorem 3.2. *The DFE, $\mathcal{E}_0$, of system (2.3) without the relative rate of infectiousness of exogenously re-infected humans ($\Theta_{RT} = 0$), the relative rates at which humans with latent schistosomiasis ($\eta_1 = 0$) and active schistosomiasis ($\eta_2 = 0$) are infected with TB, respectively and the reduced rate of re-infection with schistosomiasis ($\psi = 0$) is globally asymptotically stable (GAS) on the condition that $\mathcal{R}_{TS} < 1$ and unstable on the condition that $\mathcal{R}_{TS} > 1$.*

Proof: In order to prove the GAS of the DFE, we employ the comparison theorem [25]. To do this, we rewrite the infected classes in (2.3) as

$$\frac{dX_1}{dt} = (F - V)X_1 - DX_1 \tag{3.17}$$

where

$$X_1 = [E_{HT}, I_{HT}, E_{HS}, I_{HS}, E_{TS}, I_{ST}, E_{ST}, I_{TS}, I_S, L, J]^T$$

That is,

$$\begin{pmatrix} \dot{E}_{HT} \\ \dot{I}_{HT} \\ \dot{E}_{HS} \\ \dot{I}_{HS} \\ \dot{E}_{TS} \\ \dot{I}_{ST} \\ \dot{E}_{ST} \\ \dot{I}_{TS} \\ \dot{I}_S \\ \dot{L} \\ \dot{J} \end{pmatrix} = (F - V) \begin{pmatrix} E_{HT} \\ I_{HT} \\ E_{HS} \\ I_{HS} \\ E_{TS} \\ I_{ST} \\ E_{ST} \\ I_{TS} \\ I_S \\ L \\ J \end{pmatrix} - D \begin{pmatrix} E_{HT} \\ I_{HT} \\ E_{HS} \\ I_{HS} \\ E_{TS} \\ I_{ST} \\ E_{ST} \\ I_{TS} \\ I_S \\ L \\ J \end{pmatrix}, \tag{3.18}$$

where

$$F = \begin{pmatrix} F_{11(6\times6)} & F_{12(6\times5)} \\ F_{21(5\times6)} & F_{22(5\times5)} \end{pmatrix}, \tag{3.19}$$

$$F_{11} = \begin{pmatrix} 0 & 0 & 0 & 0 & 0 & 0 \\ \kappa_1 & \beta_T & 0 & 0 & 0 & 0 \\ 0 & 0 & 0 & 0 & 0 & 0 \\ 0 & 0 & 0 & 0 & 0 & 0 \\ 0 & 0 & 0 & 0 & 0 & 0 \\ 0 & 0 & 0 & 0 & \kappa_2 & 0 \end{pmatrix}, \quad F_{12} = \begin{pmatrix} 0 & 0 & 0 & 0 & 0 \\ 0 & \beta_T \Pi_2 & 0 & 0 & 0 \\ 0 & 0 & 0 & 0 & \frac{\beta_J \Lambda_H}{J_0 \mu_H} \\ 0 & 0 & 0 & 0 & 0 \\ 0 & 0 & 0 & 0 & 0 \\ 0 & 0 & 0 & 0 & 0 \end{pmatrix}, \tag{3.20}$$

$$F_{21} = \begin{pmatrix} 0 & 0 & 0 & 0 & 0 & 0 \\ 0 & 0 & 0 & 0 & 0 & 0 \\ 0 & 0 & 0 & 0 & 0 & 0 \\ 0 & 0 & 0 & 0 & 0 & 0 \\ 0 & 0 & 0 & 0 & 0 & 0 \end{pmatrix}, \quad F_{22} = \begin{pmatrix} 0 & 0 & 0 & 0 & 0 \\ \kappa_3 & 0 & 0 & 0 & 0 \\ 0 & 0 & 0 & \frac{\beta_L \Lambda_S}{L_0 \mu_S} & 0 \\ 0 & 0 & 0 & 0 & 0 \\ 0 & 0 & 0 & 0 & 0 \end{pmatrix}. \tag{3.21}$$

$$V = \begin{pmatrix} V_{11(6\times6)} & V_{12(6\times5)} \\ V_{21(5\times6)} & V_{22(5\times5)} \end{pmatrix}, \tag{3.22}$$

where

$$V_{11} = \begin{pmatrix} M_1^{'} & 0 & 0 & 0 & 0 & 0 \\ 0 & M_2^{'} & 0 & 0 & 0 & 0 \\ 0 & 0 & M_3^{'} & 0 & 0 & 0 \\ 0 & 0 & -\alpha_1 & M_4^{'} & 0 & 0 \\ 0 & 0 & 0 & 0 & M_5^{'} & 0 \\ 0 & 0 & 0 & 0 & 0 & M_6^{'} \end{pmatrix}, \tag{3.23}$$

$$V_{12} = \begin{pmatrix} 0 & 0 & 0 & 0 & 0 \\ 0 & 0 & 0 & 0 & 0 \\ 0 & 0 & 0 & 0 & 0 \\ 0 & 0 & 0 & 0 & 0 \\ 0 & 0 & 0 & 0 & 0 \\ 0 & 0 & 0 & 0 & 0 \end{pmatrix}, \tag{3.24}$$

$$V_{21} = \begin{pmatrix} 0 & 0 & 0 & 0 & -\alpha_2 & 0 \\ 0 & 0 & 0 & 0 & 0 & 0 \\ 0 & 0 & 0 & 0 & 0 & 0 \\ 0 & 0 & 0 & -N_e\gamma & 0 & 0 \\ 0 & 0 & 0 & 0 & 0 & 0 \end{pmatrix}, \quad V_{22} = \begin{pmatrix} M_7^{'} & 0 & 0 & 0 & 0 \\ 0 & M_8^{'} & 0 & 0 & 0 \\ 0 & 0 & M_9^{'} & 0 & 0 \\ -N_e\gamma & -N_e\gamma & 0 & M_{10}^{'} & 0 \\ 0 & 0 & -\phi & 0 & M_{11}^{'} \end{pmatrix} \tag{3.25}$$

with $M_1^{'} = \kappa_1 + \mu_H$, $M_2^{'} = \delta_T + \mu_H$, $M_3^{'} = \alpha_1 + \mu_H$, $M_4^{'} = \delta_S + \mu_H$, $M_5^{'} = \alpha_2 + \kappa_2 + \mu_H$, $M_6^{'} = \sigma + \chi_1\delta_T + \mu_H$, $M_7^{'} = \kappa_3 + v_1\delta_S + \mu_H$, $M_8^{'} = \chi_2\delta_T + v_3\delta_S + \mu_H$,

$M_9^{'} = \mu_S$, $M_{10}^{'} = \mu_L$, and $M_{11}^{'} = \mu_J$.
And

$$D = \begin{pmatrix} D_{11(6\times6)} & D_{12(6\times5)} \\ D_{21(5\times6)} & D_{22(5\times5)} \end{pmatrix}, \tag{3.26}$$

where

$$D_{11} = \begin{pmatrix} 0 & 0 & 0 & 0 & 0 & 0 \\ \kappa_1 G_1 & \beta_T G_1 & 0 & 0 & 0 & 0 \\ 0 & 0 & 0 & 0 & 0 & 0 \\ 0 & 0 & 0 & 0 & 0 & 0 \\ 0 & 0 & 0 & 0 & 0 & 0 \\ 0 & 0 & 0 & 0 & 0 & 0 \end{pmatrix}, \qquad D_{12} = \begin{pmatrix} 0 & 0 & 0 & 0 & 0 \\ 0 & \beta_T \Pi_2 G_1 & 0 & 0 & 0 \\ 0 & 0 & 0 & 0 & \beta_J J G_2 \\ 0 & 0 & 0 & 0 & 0 \\ 0 & 0 & 0 & 0 & 0 \\ 0 & 0 & 0 & 0 & 0 \end{pmatrix}, \tag{3.27}$$

$$D_{21} = \begin{pmatrix} 0 & 0 & 0 & 0 & 0 & 0 \\ 0 & 0 & 0 & 0 & 0 & 0 \\ 0 & 0 & 0 & 0 & 0 & 0 \\ 0 & 0 & 0 & 0 & 0 & 0 \\ 0 & 0 & 0 & 0 & 0 & 0 \end{pmatrix}, \qquad D_{22} = \begin{pmatrix} 0 & 0 & 0 & 0 & 0 \\ 0 & 0 & 0 & 0 & 0 \\ 0 & 0 & 0 & \beta_L L G_3 & 0 \\ 0 & 0 & 0 & 0 & 0 \\ 0 & 0 & 0 & 0 & 0 \end{pmatrix} \tag{3.28}$$

and

$$G_1 = 1 - \frac{S_H}{N_H}, \quad G_2 = \frac{\Lambda_H}{J_0 \mu_H} - \frac{S_H}{J_0 + \epsilon J}, \quad G_3 = \frac{\Lambda_S}{L_0 \mu_S} - \frac{S_S}{L_0 + \epsilon L} \tag{3.29}$$

which implies that $D \geq 0$ since, $S_H \leq N_H \leq \Lambda_H/\mu_H$, $\frac{S_H}{J_0+\epsilon J} \leq \frac{\Lambda_H}{J_0 \mu_H}$, and since $S_S \leq N_S \leq \Lambda_S/\mu_S$, $\frac{S_S}{L_0+\epsilon L} \leq \frac{\Lambda_S}{L_0 \mu_S}$ for $t > 0$ in $\mathcal{D}$. It, therefore, follows that

$$\begin{pmatrix} \dot{E}_{HT} \\ \dot{I}_{HT} \\ \dot{E}_{HS} \\ \dot{I}_{HS} \\ \dot{E}_{TS} \\ \dot{I}_{ST} \\ \dot{E}_{ST} \\ \dot{I}_{TS} \\ \dot{I}_{S} \\ \dot{L} \\ \dot{J} \end{pmatrix} \leq (F-V) \begin{pmatrix} E_{HT} \\ I_{HT} \\ E_{HS} \\ I_{HS} \\ E_{TS} \\ I_{ST} \\ E_{ST} \\ I_{TS} \\ I_{S} \\ L \\ J \end{pmatrix}, \tag{3.30}$$

Using the phenomenon that the eigenvalues of the matrix $F - V$ possess negative real components (see local stability consequence, when $\rho(FV^{-1}) < 1$ on the condition that $\mathcal{R}_{TS} < 1$ which is commensurate with $F - V$ possessing eigenvalues with negative real components whenever $\mathcal{R}_{TS} < 1$ [56]), it ensues that the linearised differential inequality system (3.30) is stable whenever $\mathcal{R}_{TS} < 1$. Consequently, $(E_{HT}, I_{HT}, E_{HS}, I_{HS}, E_{TS}, I_{ST}, E_{ST}, I_{TS}, I_S, L, J) \to (0,0,0,0,0,0,0,0,0,0,0)$ as $t \to \infty$. Thus, by the comparison theorem in [25] $(E_{HT}, I_{HT}, E_{HS}, I_{HS}, E_{TS}, I_{ST}, E_{ST}, I_{TS}, I_S, L, J) \to (0,0,0,0,\ 0,0,0,0,0,0,0)$ as $t \to \infty$. Substituting $E_{HT} = I_{HT} = E_{HS} = I_{HS} = E_{TS} = I_{ST} = E_{ST} = I_{TS} = I_S = L = J = 0$ in the special case of equation (2.3) gives $S_H(t) \to S_H^*$, $S_S(t) \to S_S^*$, as $t \to \infty$. Thus, $(S_H, E_{HT}, I_{HT}, E_{HS}, I_{HS}, E_{TS}, I_{ST}, E_{ST}, I_{TS}, L, S_S, I_S, J) \to (S_H^*, 0,0,0,0,0,0,0,0,0,0, S_S^*, 0, 0)$ as $t \to \infty$ for $\mathcal{R}_{TS} < 1$. Thus, $\mathcal{E}_0$, is globally asymptotically stable if $\mathcal{R}_{TS} < 1$ when $\Theta_{RT} = \eta_1 = \eta_2 = \psi = 0$.

4 Numerical Simulations

The system (2.3) is simulated, numerically, in order to investigate the impact of varying certain critical parameters describing the relative infectiousness of humans

with latent and active schistosomiasis, the relative infectiousness of exogenously re-infected humans, the reduced re-infection with schistosomiasis and reinfection exogenous-wise on the population dynamics of TB-schistosomiasis co-infection. In the numerical simulations carried out in this section, we used specific demographic and epidemiological characteristics pertinent to Nigeria (*see* Table 2 and Table 3, respectively). In 2017, the total population of Nigeria was estimated to be 189,559,502 [15] . Hence, it follows that, at the DFE, $\Lambda_H/\mu_H = 189,559,502$. The mean mortality rate per year in Nigeria is $\mu_H = 0.02041$ [55]. Hence, the average recruitment rate into the population is $\Lambda_H = 3,868,900$ per year. Moreover, in 2017, the total incidence of TB in Nigeria was estimated to be 407,000 [61] while the total incidence of schistosomiasis in Nigeria was approximately 29,000,000 [61].

Figure 1 shows the cumulative TB incidence when the rate of relative infectiousness of humans with latent schistosomiasis (η_1) was varied from 0 to 2. The simulation reveals that the frequency of TB increased as the rate of relative infectiousness of humans with latent schistosomiasis increases (i.e., $\eta_1 \to 2$) amongst human individuals with active schistosomiasis as in Figure 1(b). The result of simulation shows that the frequency of TB in a population could increase as the rate of relative infectiousness of humans with latent schistosomiasis increases. Reducing the rate of relative infectiousness of humans with latent schistosomiasis (i.e., $\eta_1 \to 0$) as a control strategy could result in the avoidance of about 12, 960 cases of new TB infections.

Figure 2 shows the cumulative TB frequency when the rate of relative infectiousness of humans with active schistosomiasis (η_2) was varied from 0 to 4. The simulation reveals that the frequency of TB increased as the rate of relative infectiousness of humans with active schistosomiasis increases (i.e., $\eta_2 \to 4$) amongst human individuals with active schistosomiasis as in Figure 2(b). The outcome of the simulation shows that the frequency of TB in a population could increase as the rate of with active schistosomiasis increases. Reducing the of relative infectiousness of humans with active schistosomiasis (i.e., $\eta_2 \to 0$) as a control strategy could result in the prevention of about 27, 670 cases of new TB

Table 2: Parameter values (and ranges) of the model system (2.3)

Parameters	Values	Sample ranges	References
μ_H	0.02041 year^{-1}	[0.0143, 0.03]	[55]
Λ_H	3 868 900 year^{-1}	[3,000,000, 4,000,000]	[15]
β_T	Variable year^{-1}	[0, 2]	[60]
ξ	0.075 year^{-1}	[0, 1]	[19]
p	0.1 year^{-1}	[0, 1]	Assumed
f	0.1 year^{-1}	[0, 0.005]	[47]
m	0.1 year^{-1}	[0, 3]	[47]
π_1	0.4 year^{-1}	[0, 1]	[19]
π_2	0.45 year^{-1}	[0, 1]	[19]
π_3	0.5 year^{-1}	[0, 1]	[19]
k_1	0.005 year^{-1}	[0.005, 0.05]	[7]
k_2	0.005 year^{-1}	[0.005, 0.05]	[7]
k_3	0.005 year^{-1}	[0.005, 0.05]	[7]
ζ_T	0.75 year^{-1}	[0.5, 1]	[36]
ζ_{T1}	0.75 year^{-1}	[0.5, 1]	[36]
ζ_{T2}	0.75 year^{-1}	[0.5, 1]	[36]
ζ_{T3}	0.75 year^{-1}	[0.5, 1]	[36]
ζ_R	0.75 year^{-1}	[0.5, 1]	[36]
ζ_{R1}	0.75 year^{-1}	[0.5, 1]	[36]
ζ_S	0.23 year^{-1}	[0.23, 0.49]	[22]
ζ_{S1}	0.23 year^{-1}	[0.23, 0.49]	[22]
ζ_{S2}	0.23 year^{-1}	[0.23, 0.49]	[22]
ζ_{S3}	0.23 year^{-1}	[0.23, 0.49]	[22]

infections.

Figure 3 shows the cumulative TB frequency when the rate of relative

Table 3: Parameter values (and ranges) of the model system (2.3) (cont'd)

Parameters	Values	Sample ranges	References
δ_T	0.1 year^{-1}	[0, 0.5]	[6]
δ_R	0.1 year^{-1}	[0, 0.5]	[6]
δ_S	1.4 year^{-1}	[0.365, 2.19]	[32]
α_1	6.5 year^{-1}	[0, 10]	[32]
α_2	6.5 year^{-1}	[0, 10]	[32]
α_3	6.5 year^{-1}	[0, 10]	[32]
ψ	0.85 year^{-1}	[0.05, 0.85]	Assumed
σ	0.5 year^{-1}	[0, 1]	Assumed
χ_1	0.65 year^{-1}	[0, 1]	Assumed
χ_2	0.85 year^{-1}	[0, 1]	Assumed
η_1	2.0 year^{-1}	[0, 3]	Assumed
η_2	4.0 year^{-1}	[0, 5]	Assumed
Θ_{RT}	0.5 year^{-1}	[0, 1]	Assumed
Θ_{RS1}	1.5 year^{-1}	[0, 3]	Assumed
Θ_{RS2}	1.5 year^{-1}	[0, 3]	Assumed
Π_1	1.8 year^{-1}	[0, 3]	Assumed
Π_2	2.0 year^{-1}	[0, 3]	Assumed
v_1	0.001 year^{-1}	[0, 1]	Assumed
v_2	0.002 year^{-1}	[0, 1]	Assumed
v_3	0.003 year^{-1}	[0, 1]	Assumed
μ_S	0.5 year^{-1}	[0, 1]	[22]
Λ_S	73,000 year^{-1}	[73,000, 109,500]	[13]
ϵ	182.5 year^{-1}	[0, 182.5]	[13]
β_L	1.475 year^{-1}	[0, 2]	Assumed
L_0	10^8 year^{-1}	[9×10^7, 1×10^8]	[13]
N_e	300 year^{-1}	[0, 800]	[13]
γ	0.8468 year^{-1}	[0, 1]	[13]
μ_L	328.5 year^{-1}	[100, 400]	[13]
β_J	4.19 year^{-1}	[0, 5]	Assumed
J_0	9×10^7 year^{-1}	[8×10^7, 9×10^7]	[13]
μ_J	3.0 year^{-1}	[0, 3]	[13]
τ_1	0.1 year^{-1}	[0, 1]	Assumed
τ_2	0.2 year^{-1}	[0, 1]	Assumed
ϕ	500 year^{-1}	[0, 1,000]	[13]

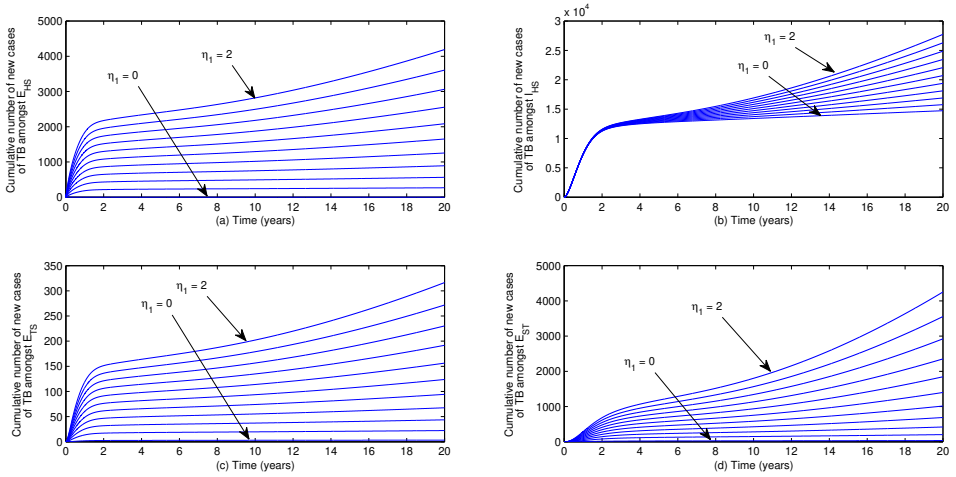

Figure 1: Cumulative number of new TB cases with $\beta_T = 1.2$, and varied rate of relative infectiousness of humans with latent schistosomiasis (η_1).

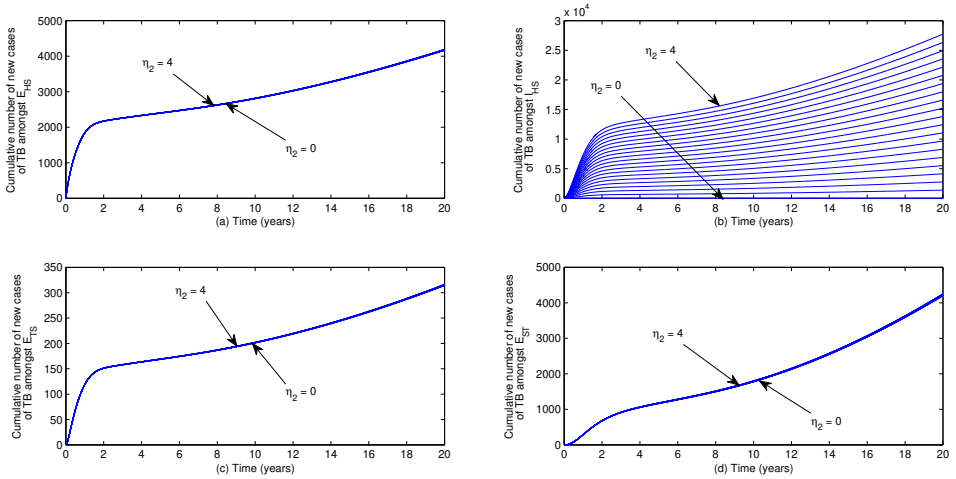

Figure 2: Cumulative number of new TB cases with $\beta_T = 1.2$, and varied rate of relative infectiousness of humans with active schistosomiasis (η_2).

infectiousness of exogenously re-infected humans with TB (Θ_{RT}) was varied from 0 to 1. The simulation reveals that the frequency of TB increased as the rate of relative rate of infectiousness of exogenously re-infected humans with TB increases (i.e., $\Theta_{RT} \to 1$) amongst human individuals active schistosomiasis as in Figure 3(b). The simulation result shows that the frequency of TB in a population could increase as the relative rate of infectiousness of exogenously re-infected humans with TB increases. Reducing the relative rate of infectiousness of exogenously re-infected humans with TB (i.e., $\Theta_{RT} \to 0$) as a control strategy could result in the prevention of about 530 cases of new TB infections.

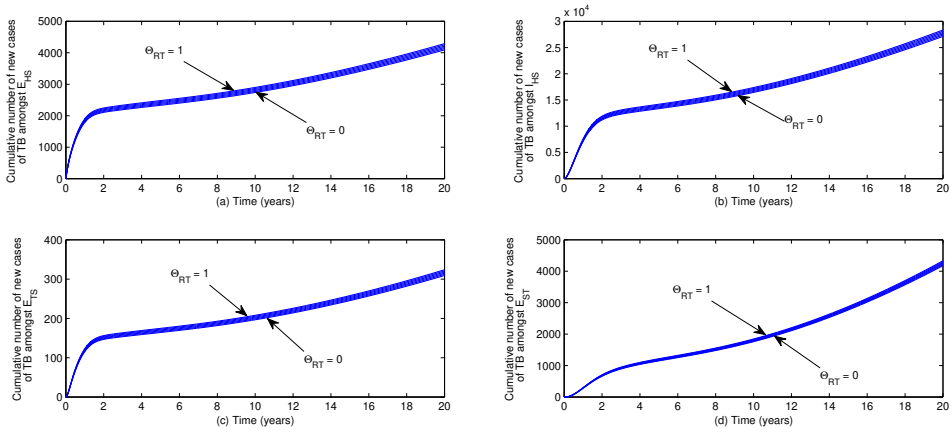

Figure 3: Cumulative number of new TB cases with $\beta_T = 1.2$, and varied relative rate of infectiousness of exogenously re-infected humans with TB (Θ_{RT}).

When the rate of cercarial generation in the aquatic environment (ϕ) is changed from 200 to 1,000, Figure 4 displays the cumulative TB incidence. The simulation's result indicates that when the rate of cercarial development in an aquatic environment increases, the frequency of tuberculosis (TB) increases (i.e., $\phi \to 1,000$) amongst human individuals with active schistosomiasis as in Figure 4(b). The result of the simulation shows that the frequency of TB in a population could increase as the rate of cercarial production in the aquatic environment increases. Reducing the rate of cercarial production in the aquatic setting (i.e.,

$\phi \to 200$) as a control strategy could result in the prevention of about 31, 240 cases of new TB infections.

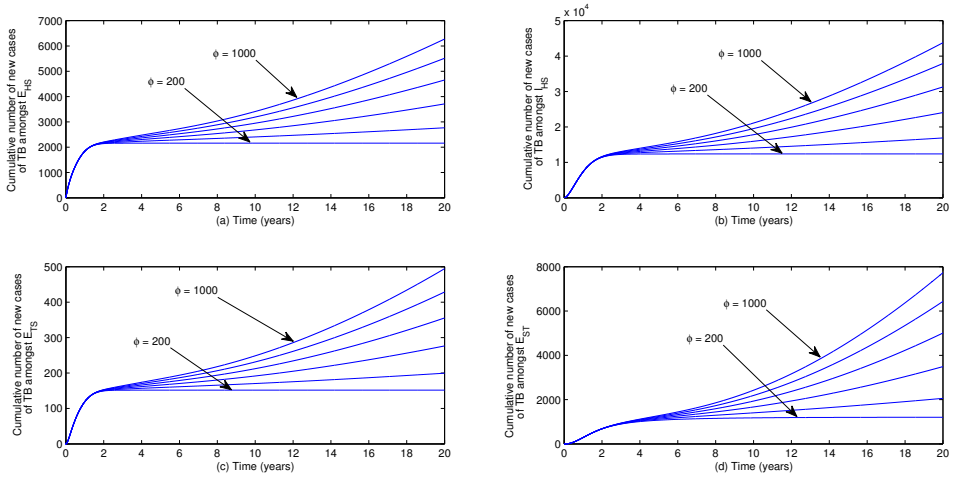

Figure 4: Cumulative number of new TB cases with $\beta_T = 1.2$, and varied rate of cercarial production in the aquatic environment (ϕ).

5 Conclusions

To investigate how the relative infectiousness of TB-infected individuals who become active through exogenous re-infection affects the total TB burden in the population, a unique deterministic mathematical model is created. The following is a summary and availability of the main findings: It was shown that the disease-free state was locally asymptotically stable (LAS) when the related effective reproduction number of the model (2.3) was less than unity. Furthermore, the model was shown to illustrate the backward bifurcation phenomenon caused by the relative rate of infectiousness (Θ_{RT}) of the exogenously re-infected individuals, which represents the percentage of individuals who rapidly progress to active tuberculosis (p), the relative rates at which humans with latent

schistosomiasis (η_1) and active schistosomiasis (η_2) contract tuberculosis, and the decreased rate of schistosomiasis re-infection (ψ), the adjustment parameter which accounts for the increased probability of infectiousness of humans with active TB and latent schistosomiasis (Π_1), the treatment rate of individuals with active TB exposed to schistosomiasis (ζ_{T1}) and the rate of progression to active TB/exposed to schistosomiasis to active TB/active schistosomiasis (σ) induce backward bifurcation in the disease dynamics of TB in the presence of schistosomiasis. Additionally, a special case of the model system (2.3) was shown to be asymptotically stable globally (GAS), When the associated effective reproduction number was below unity.

This study has revealed that TB and schistosomiasis control programmes that uphold the respective treatment of active cases of both diseases and the deliberate reduction of cercarial production in the aquatic environment should be tenaciously pursued, since it has been shown that such programmes have the propensity to result in significant decline in the burden of TB-schistosomiasis co-infection in the populace. Also, to prevent the situation where the backward bifurcation phenomenon may occur, control measures should target the following parameters that are responsible for its occurrence, namely: the relative rate of infectiousness of exogenously re-infected humans (Θ_{RT}), the relative rates at which humans with latent schistosomiasis (η_1) and active schistosomiasis (η_2) are infected with TB, respectively and the reduced rate of re-infection with schistosomiasis (ψ), the fraction of individuals who experience fast progression to active TB (p), the adjustment parameter which accounts for the increased probability of infectiousness of humans with active TB and latent schistosomiasis (Π_1), the treatment rate of individuals with active TB exposed to schistosomiasis (ζ_{T1}) and the rate of progression to active TB/exposed to schistosomiasis to active TB/active schistosomiasis (σ).

The incidence of TB-schistosomiasis co-infection in the population could be significantly reduced by lowering the value of critical parameters such as the rate of relative infectiousness of humans with latent and active schistosomiasis, respectively, the rate of infectiousness of exogenously re-infected humans with

TB combined with effective treatment, and the rate of cercarial production in the aquatic environment. These findings were obtained from the numerical simulation of the model system (2.3).

References

[1] Ako, I. I., Akhaze, R. U., & Olowu, O. O. (2021). The impact of reduced re-infection on schistosomiasis transmission dynamics at population level: a theoretical study. *Journal of the Nigerian Association of Mathematical Physics, 59*, 61-74.

[2] Andrews, J. A., Noubary, F., Walensky, R. P., Cerda, R., Losina, E., & Horsburgh, R. (2012). Risk of progression to active tuberculosis following reinfection with mycobacterium tuberculosis. *Clinical Infectious Diseases, 54*(6), 784-791. https://doi.org/10.1093/cid/cir951

[3] Athithan, S., & Ghosh, M. (2013). Mathematical modelling of TB with the effects of case detection and treatment. *International Journal of Dynamics and Control, 1*, 223-230. https://doi.org/10.1007/s40435-013-0020-2

[4] Barbour, A.D. (1982). Schistosomiasis. In R.M. Anderson (Ed.), *Population dynamics of infectious diseases* (pp. 180-208). Chapman and Hall. https://doi.org/10.1007/978-1-4899-2901-3_6

[5] Bhunu, C. P. (2011). Mathematical analysis of a three-strain tuberculosis transmission model. *Applied Mathematical Modelling, 35*(35), 4647-4660. https://doi.org/10.1016/j.apm.2011.03.037

[6] Bhunu, C. P., Garira, W., & Magombedze, G. (2009). Mathematical analysis of a two-strain HIV/AIDS model with antiretroviral treatment. *Acta Biotheoretica, 57*(3), 361-381. https://doi.org/10.1007/s10441-009-9080-2

[7] Blower, S. M., McLean, A. R., Porco, T. C., Small, P. M., Hopwell, P. C., Sanchez, M. A., & Moss, A. R. (1995). The intrinsic transmission dynamics of tuberculosis epidemics. *Nature Medicine, 1*, 815-821. https://doi.org/10.1038/nm0895-815

[8] Castillo-Chavez, C., Feng, Z., & Xu, D. (2008). A schistosomiasis model with mating structure and time delay. *Mathematical Biosciences, 211*, 333-341. https://doi.org/10.1016/j.mbs.2007.11.001

[9] Castillo-Chavez, C., & Song, B. (2004). Dynamical models of tuberculosis and their applications. *Mathematical Biosciences and Engineering, 1*(2), 361-404. https://doi.org/10.3934/mbe.2004.1.361

[10] Chatterjee, S., & Nutman, T. B. (2015). Helminth-induced immune regulation: implications for immune responses to tuberculosis. *PLoS Pathogens, 11*(1), e1004582. https://doi.org/10.1371/journal.ppat.1004582

[11] Chen, Z., Zou, L., Shen, D., Zhang, W., & Ruan, S. (2010). Mathematical modelling and control of schistosomiasis in Hubei Province, China. *Acta Tropica, 115*, 119-125. https://doi.org/10.1016/j.actatropica.2010.02.012

[12] Chitsulo, L., Engels, D., Montresor, A., & Savioli, L. (2000). The global status of schistosomiasis and its control. *Acta Tropica, 77*, 41-51. https://doi.org/10.1016/S0001-706X(00)00122-4

[13] Chiyaka, E., & Garira, W. (2009). Mathematical analysis of the transmission dynamics of schistosomiasis in the human-snail hosts. *Journal of Biological Systems, 17*, 397-423. https://doi.org/10.1142/S0218339009002910

[14] Cohen, J.E. (1977). Mathematical models of schistosomiasis. *Annual Review of Ecology and Systematics, 8*, 209-233. https://doi.org/10.1146/annurev.es.08.110177.001233

[15] Countrymeters. (2017). Nigeria Population. Retrieved from https://countrymeters.info/en/Nigeria (accessed on July 19, 2018).

[16] Desaleng, D., & Koya, P. R. (2016). Modeling and analysis of multi-drug-resistant tuberculosis in densely populated areas. *American Journal of Applied Mathematics, 4*(1), 1-10. https://doi.org/10.11648/j.ajam.20160401.11

[17] Diaby, M. A., & Iggidr, A. (2016). A mathematical analysis of a model with mating structure. *Proceedings of CARI, 246*, 402-411.

[18] Diaby, M. A., Iggidr, A., Sy, M., & Sene, A. (2014). Global analysis of a schistosomiasis infection model with biological control. *Applied Mathematics and Computation, 246*, 731-742. https://doi.org/10.1016/j.amc.2014.08.061

[19] Feng, Z., Castillo-Chavez, C., & Capurro, A. F. (2000). A model for tuberculosis with exogenous reinfection. *Theoretical Population Biology, 57*, 235-247. https://doi.org/10.1006/tpbi.2000.1451

[20] Feng, Z., Curtis, J., & Minchella, D. J. (2001). The influence of drug treatment on the maintenance of schistosome genetic diversity. *Journal of Mathematical Biology, 43*, 52-68. https://doi.org/10.1007/s002850100092

[21] Feng, Z., Li, C.-C., & Milner, F. A. (2002). Schistosomiasis models with density dependence and age of infection in snail dynamics. *Mathematical Biosciences, 177-178*, 271-286. https://doi.org/10.1016/S0025-5564(01)00115-8

[22] Feng, Z., Eppert, A., Milner, F. A., & Minchella, D . J. (2004). Estimation of parameters governing the transmission dynamics of schistosomes. *Applied Mathematics Letters, 17*, 1105-1112. https://doi.org/10.1016/j.aml.2004.02.002

[23] Hethcote, H. W. (2000). The mathematics of infectious diseases. *SIAM Review, 42*(4), 599-653. https://doi.org/10.1137/S0036144500371907

[24] Inobaya, M. T., Olveda, R. M., Chau, T. N. P., Olveda D. U., & Ross A. G. P. (2014). Prevention and control of schistosomiasis: a current perspective. *Research and Reports in Tropical Medicine, 5*, 65-75. https://doi.org/10.2147/RRTM.S44274

[25] Lakshmikantham, V., Leela, S., & Martynyuk, A. A. (1991). Stability analysis of nonlinear systems. *SIAM Review, 33*(1), 152-154. https://doi.org/10.1137/1033038

[26] Li, X. X., & Zhou, X. N. (2013). Coinfection of tuberculosis and parasitic diseases in humans: a systematic review. *Parasites & Vectors, 6*, 79. https://doi.org/10.1186/1756-3305-6-79

[27] Macdonald, G. (1965). The dynamics of Helminth infections with special reference to schistosomes. *Transactions of the Royal Society of Tropical Medicine and Hygiene, 59*(5), 489-506. https://doi.org/10.1016/0035-9203(65)90152-5

[28] Milner, F. A., & Zhao, R. (2008). A deterministic model of schistosomiasis with spatial structure. *Mathematical Biosciences and Engineering, 5*(3), 505-522. [http://www.mbejournal.org/] https://doi.org/10.3934/mbe.2008.5.505

[29] Monin, L., Griffiths, K. L., Lam, W. Y., Gopal, R., Kang, D. D., Ahmed, M., Rajamanickam, A., Cruz-Lagunas, A., Zuniga, J., Babu, S., Kolls, J. K., Mitreva, M., Rosa, B. A., Ramos-Payan, R., Morrison, T. E., Murray, P. J., Rangel-Moreno, J., Pearce, E. J., & Khader, S. A. (2015). Helminth-induced arginase-1 exacerbates lung inflammation and disease severity in tuberculosis. *The Journal of Clinical Investigation, 125*(12), 4699-4713. https://doi.org/10.1172/JCI77378

[30] Moualeu, D. P., Weiser, M., Ehrig, R., et al. (2015). Optimal control for tuberculosis model with undetected cases in Cameroon. *Communications in Nonlinear Science and Numerical Simulation, 20*, 986-1003 https://doi.org/10.1016/j.cnsns.2014.06.037

[31] Mushayabasa, S., & Bhunu, C. P. (2011). Modeling schistosomiasis and HIV/AIDS dynamics. *Computational and Mathematical Methods in Medicine, 2011*, Article ID 846174. https://doi.org/10.1155/2011/846174

[32] Ngarakana-Gwasira, E. T., Bhunu, C. P., Masocha, M., & Mashonjowa, E. (2016). Transmission dynamics of schistosomiasis in Zimbabwe: a mathematical and GIS approach. *Communications in Nonlinear Science and Numerical Simulation, 35*, 137-147. https://doi.org/10.1016/j.cnsns.2015.11.005

[33] Okosun, K. O., & Smith?, R. (2017). Optimal control analysis of malaria-schistosomiasis co-infection dynamics. *Mathematical Biosciences & Engineering, 14*(2), 377-405. https://doi.org/10.3934/mbe.2017024

[34] Okuonghae, D. (2013). A mathematical model of tuberculosis transmission with heterogeneity in disease susceptibility and progression under a treatment regime for infectious cases. *Applied Mathematical Modelling, 37*, 6786-6808. https://doi.org/10.1016/j.apm.2013.01.039

[35] Okuonghae, D. (2014). Lyapunov functions and global properties of some tuberculosis models. *Journal of Applied Mathematics and Computing*. https://doi.org/10.1007/s12190-014-0811-4

[36] Okuonghae, D., & Aihie, V. (2008). Case detection and direct observation therapy strategy (DOTS) in Nigeria: its effect on TB dynamics. *Journal of Biological Systems, 16*(1), 1-31. https://doi.org/10.1142/S0218339008002344

[37] Okuonghae, D., & Aihie, V. U. (2010). Optimal control measures for tuberculosis mathematical models including immigration and isolation of infective. *Journal of Biological Systems, 18*(01), 17-54. https://doi.org/10.1142/S0218339010003160

[38] Okuonghae, D., & Ikhimwin, B. O. (2016). Dynamics of a mathematical model for tuberculosis with variability in susceptibility and disease progressions due to difference in awareness level. *Frontiers in Microbiology, 6*, 1530. https://doi.org/10.3389/fmicb.2015.01530

[39] Okuonghae, D., & Korobeinikov, A. (2007). Dynamics of tuberculosis: the effect of direct observation therapy strategy (DOTS) in Nigeria. *Mathematical Modelling of Natural Phenomena, 2*(1), 101-113. https://doi.org/10.1051/mmnp:2008013

[40] Okuonghae, D., & Omosigho, S.E. (2011). Analysis of a mathematical model for tuberculosis: What could be done to increase case detection. *Journal of Theoretical Biology, 269*, 31-45. https://doi.org/10.1016/j.jtbi.2010.09.044

[41] Olowu, O., & Ako, I. (2023). Computational investigation of the impact of availability and efficacy of control on the transmission dynamics schistosomiasis. *International Journal of Mathematical Trends and Technology, 69*(8), 1-9. https://doi.org/10.14445/22315373/IJMTT-V69I8P501

[42] Olowu, O., Ako, I. I., & Akhaze, R. I. (2021). Theoretical study of a two patch metapopulation schistosomiasis model. *Transactions of the Nigerian Association Mathematical Physics, 14*, 53-68.

[43] Olowu, O., Ako, I. I., & Akhaze, R. I. (2021b). On the analysis of a two patch schistosomiasis model. *Transactions of the Nigerian Association Mathematical Physics, 14*, 69-78.

[44] Omame, A., Umana, R.A., Okuonghae, D., & Inyama, S.C. (2018). Mathematical analysis of a two-sex human papillomavirus (HPV) model. *Int. J. Biol., 11*(7). https://doi.org/10.1142/S1793524518500924

[45] Osada, Y., & Kanazawa, T. (2011). Schistosome: Its benefit and harm in patients suffering from concomitant diseases. *Journal of Biomedicine and Biotechnology, 2011*. https://doi.org/10.1155/2011/264173

[46] Pangaribuan, R.M., et al. (2016). Threshold dynamic for quasi-endemic equilibrium from co-epidemic HIV-TB model with re-infection TB in heterosexual population.

International Conference on Mathematics, Engineering and Industrial Applications, 030041. https://doi.org/10.1063/1.4965161

[47] Porco, T.C., & Blower, S.M. (1998). Quantifying the intrinsic transmission dynamics of tuberculosis. *Theor Pop Biol, 54*, 117-132. https://doi.org/10.1006/tpbi.1998.1366

[48] Potian, J.A., Rafi, W., Bhatt, K., McBride, A., Gause, W.C., & Salgame, P. (2011). Preexisting helminth infection induces inhibition of innate pulmonary anti-tuberculosis defense by engaging the IL-4 receptor pathway. *J. Exp. Med., 208*(9), 1863-1874. https://doi.org/10.1084/jem.20091473

[49] Qi, L., & Cui, J. (2013). A schistosomiasis model with mating structure. *Abstract and Applied Analysis, 2013*. https://doi.org/10.1155/2013/741386

[50] Qi, L., et al. (2014). Mathematical model of schistosomiasis under flood in Anhui Province. *Abstract and Applied Analysis, 2014*. https://doi.org/10.1155/2014/972189

[51] Qi, L., et al. (2018). Schistosomiasis model and its control in Anhui Province. *Bulletin of Mathematical Biology, 80*, 2435-2451. https://doi.org/10.1007/s11538-018-0474-7

[52] Sharomi, O., & Malik, T. (2017). A model to assess the effect of vaccine compliance on human papillomavirus infection and cervical cancer. *Appl. Math. Model., 47*, 528-550. https://doi.org/10.1016/j.apm.2017.03.025

[53] Sharomi, O., Podder, C.N., & Gumel, A.B. (2008). Mathematical analysis of the transmission dynamics of HIV/TB co-infection in the presence of treatment. *Math. Biosci. Eng., 5*(1), 145-174. https://doi.org/10.3934/mbe.2008.5.145

[54] Simon, G.G. (2016). Impacts of neglected tropical disease on incidence and progression of HIV/AIDS, tuberculosis, and malaria: scientific links. *International Journal of Infectious Diseases, 42*, 54-57. https://doi.org/10.1016/j.ijid.2015.11.006

[55] UNAIDS-WHO (2004). Epidemiological fact sheet. Retrieved from http://www.unaids.org.

[56] van den Driessche, P., & Watmough, J. (2002). Reproduction numbers and sub-threshold endemic equilibria for compartmental models of disease transmission. *Mathematical Biosciences, 180*, 29-48. https://doi.org/10.1016/S0025-5564(02)00108-6

[57] Waaler, H., Geser, A., & Andersen, S. (1962). The use of mathematical models in the study of the epidemiology of tuberculosis. *Am. J. Public Health Nations Health., 52*(6), 1002-1013. https://doi.org/10.2105/AJPH.52.6.1002

[58] WHO (World Health Organization). (2008). Global Tuberculosis Control-Surveillance, Planning, Financing. Geneva, Switzerland: WHO Press.

[59] WHO (World Health Organization). (2015). Global tuberculosis report. Geneva, Switzerland: WHO Press.

[60] WHO (World Health Organization). (2016). Global tuberculosis report 2016. Geneva, Switzerland: WHO Press.

[61] WHO (World Health Organization). (2017). Schistosomiasis Factsheet 2017. Geneva, Switzerland: WHO Press.

[62] WHO (World Health Organization). (2018). Tuberculosis Factsheet 2018. Geneva, Switzerland: WHO Press.

[63] WHO (World Health Organization). (2019). Schistosomiasis Factsheet 2019. Geneva, Switzerland: WHO Press.

[64] Woolhouse, M.E.J. (1991). On the application of mathematical models of schistosome transmission dynamics I: natural transmission. *Acta Trop., 49*, 241. https://doi.org/10.1016/0001-706X(91)90077-W

[65] Yang, H.M. (2003). Comparison between schistosomiasis transmission modeling considering acquired immunity and age-structured contact pattern with infested water. *Mathematical Biosciences, 184*, 1-26. https://doi.org/10.1016/S0025-5564(03)00045-2

[66] Zhao, R., & Milner, F.A. (2008). A mathematical model of schistosoma mansoni in *Biomphalaria glabrata* with control strategies. *Bulletin of Mathematical Biology, 70*(7), 1886-1905. https://doi.org/10.1007/s11538-008-9330-5

[67] Zou, L., & Ruan, S. (2015). Schistosomiasis transmission and control in China. *Acta Tropica, 143*, 51-57. https://doi.org/10.1016/j.actatropica.2014.12.004